International Interdisciplinary Congress on Renewable Energies, Industrial Maintenance, Mechatronics and Informatics
Booklets

RENIECYT 1702902 CONACYT

RENIECYT - LATINDEX - Research Gate - DULCINEA - CLASE - Sudoc - HISPANA - SHERPA UNIVERSIA - Google Scholar DOI - REDIB - Mendeley - DIALNET - ROAD - ORCID

Title: Photoluminescence comparison of CNTs-SRO and GO-SRO films deposited on silicon substrates

Authors: MENDOZA-CONDE, Gabriel Omar, LUNA-LÓPEZ, José Alberto, HERNÁNDEZ-SIMÓN, Zaira Jocelyn and HERNÁNDEZ-DE LA LUZ, José Álvaro David

Editorial label ECORFAN: 607-8695
BCIERMMI Control Number: 2022-01
BCIERMMI Classification (2022): 261022-0001

Pages: 8
RNA: 03-2010-032610115700-14

ECORFAN-México, S.C.
143 – 50 Itzopan Street
La Florida, Ecatepec Municipality
Mexico State, 55120 Zipcode
Phone: +52 1 55 6159 2296
Skype: ecorfan-mexico.s.c.
E-mail: contacto@ecorfan.org
Facebook: ECORFAN-México S. C.
Twitter: @EcorfanC

www.ecorfan.org

Holdings
Mexico Colombia Guatemala
Bolivia Cameroon Democratic
Spain El Salvador Republic
Ecuador Taiwan of Congo
Peru Paraguay Nicaragua

Introduction

One of the most technologically interesting materials is silicon-rich oxide (SRO), which is considered to be a material with great potential for the fabrication of optoelectronic devices because it is a material compatible with CMOS technology. In addition to various methods can be used to obtain the SRO, such as LPCVD, PEVCD, HFCVD, implantation of silicon in SiO_2, sputtering, etc. [1].

A relevant characteristic of the SRO is that it facilitates the formation of silicon nanocrystals embedded in a SiO_2 matrix [2], which generate low dimensional effects and therefore, an efficient emission of light [1]. The SRO possesses interesting structural, optical, and electrical properties which can be tailored by the silicon excess and defects contained in the films [3]. The incorporation of silicon into SiO_x modifies its bandgap as well as its optical properties such as photoluminescence, absorption and emission of light. The latter is attributed to quantum effects present in silicon nanocrystals and localized defects at the interface between nanocrystals and silicon matrix. [4].

On the other hand, carbon nanostructures such as fullerenes, carbon nanotubes (CNTs), nanodiamond (ND) films, and graphene oxide (GO) are very attractive functional groups in the fabrication of important optoelectronic devices such as sensors, field emitters, and light-emitting applications [5]. Luminescent carbon nanostructures are also expected to achieve high-efficiency photoluminescence in light-emitting devices and low toxicity in biological and biomedical applications [6].

There are two types of CNTs; single-wall carbon nanotubes (SWCNTs) and multi-wall carbon nanotubes (MWCNTs). MWCNT is a CNT structure consisting of several coaxially concentric shells of graphene sheets rolled up. In both cases, their one-dimensional structure, interlayer interaction and curvature effects lead to many extraordinary mechanical, electrical, optical, thermal and chemical properties. All of this makes them suitable for enhancing the functionalization of existing materials and even creating other heterostructures. Furthermore, CNTs thin films are electrically conductive and transparent, and have recently been used as ohmic contacts in GaN and organic materials [7], In this context, the SRO may be used to realize novel heterostructures using CNTs to improve its optical properties.

On the other hand, Graphene oxide is a bidimensional carbon-based material that can be used in graphene-based optoelectronic devices, especially for biomedical applications, due to its unique electronic properties and large specific surface area [8, 9]. Since graphene has no band gap as an intrinsic material, it is not expected to exhibit photoluminescence due to relaxation of excited carriers; however, when, it is functionalized, such as graphene oxide, it has a band gap and exhibits photoluminescence [10]. Therefore, the GO may be used to form new structures in order to enrich their optical properties.

Thus, by using CNTs and GO along with the SRO it is possible to make up nanostructured materials which may be of great interest because of their outstanding photoluminescent properties based on the quantum effects due to low dimensions and energy band structures. Thus, these photoluminescent properties may be focused on forming new light-emitting devices in the field of optoelectronics.

Methodology

CNTs and GO thin films were deposited on n-type crystalline silicon substrates with 100 orientation and <0.005 Ω-cm resistivity by the spin-coating method shown in Figure 1.

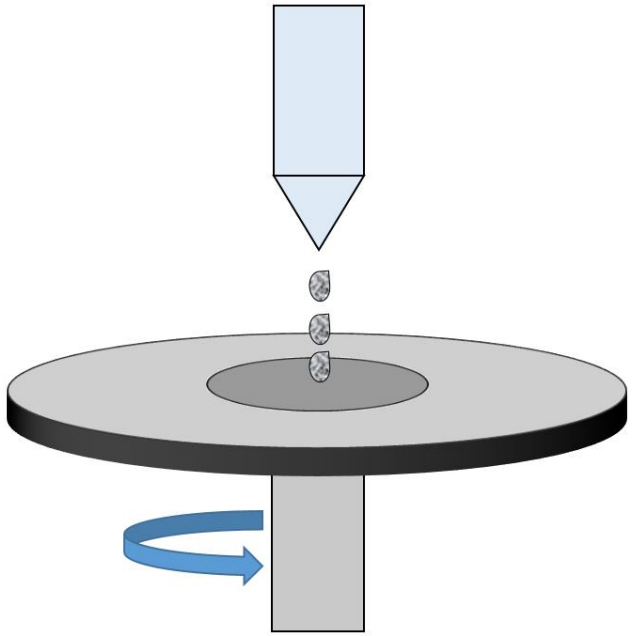

Figure 1. Spin coating process.

All structures to be deposited (CNTs and GO) are dissolved in an alcoholic solvent, in this case methanol.

The parameters used for thin film deposition are as follows: the first speed is 700 rpm for a deposition time of 10 s, and the second speed is 3000 rpm for 15 s to deposit 3 drops of the solution, using methanol as the solvent and repeat the process three times. The concentrations of CNTs and GO solutions were 1.8 g/L and 1.3 g/L, respectively.

Methodology

The SRO films were deposited on the Si/CNTs, Si/GO, Si/CNTs-GO and Si/GO-CNTs structures using a HFCVD (Hot Filament Chemical Vapor Deposition) reactor. These depositions were carried out with a constant flow of molecular hydrogen (H_2) at 100 sccm level, the source-to-substrate distance (ssd) was kept at 7 mm. Some parameters were fixed during the deposition process, such as the filament-to-source distance (fsd), which was kept constant at 8 mm, the deposition time (td) was 1 min, the voltage applied to the filaments was 84 V and the system pressure at one atmosphere.

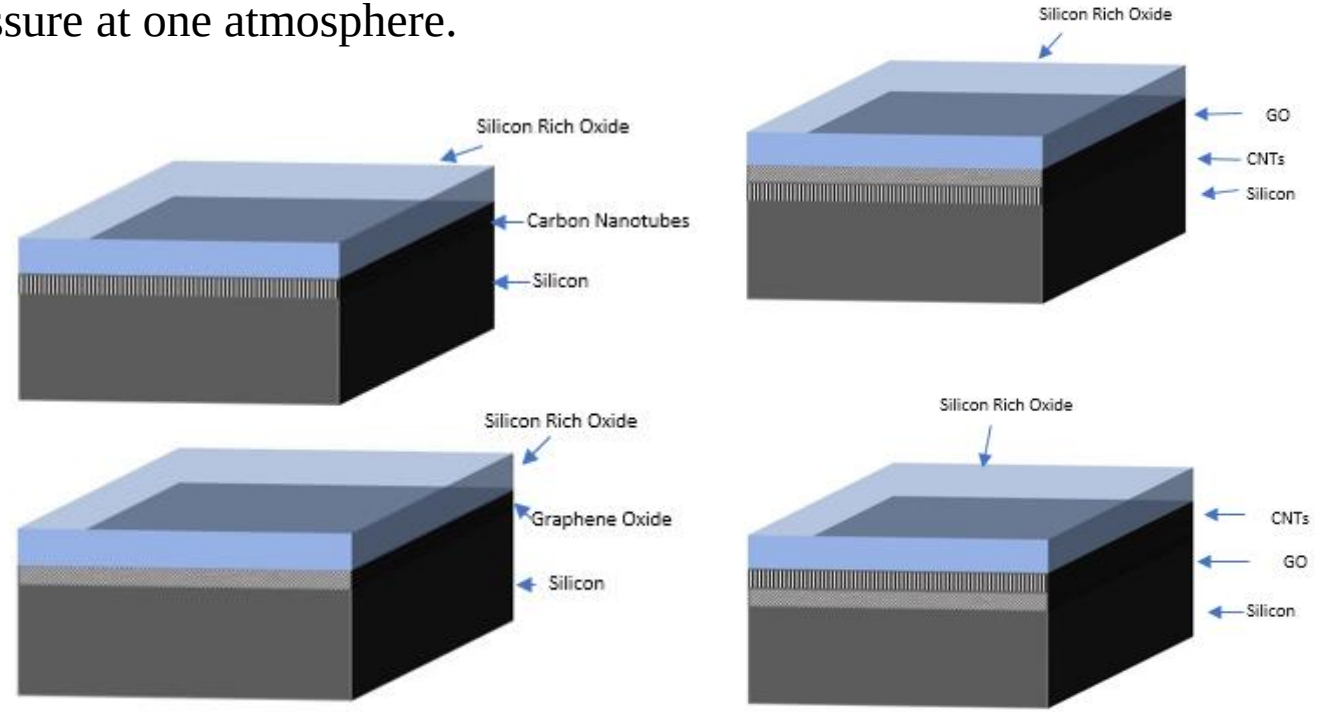

Figure 2. Scheme of the 4 manufactured structures.

Results

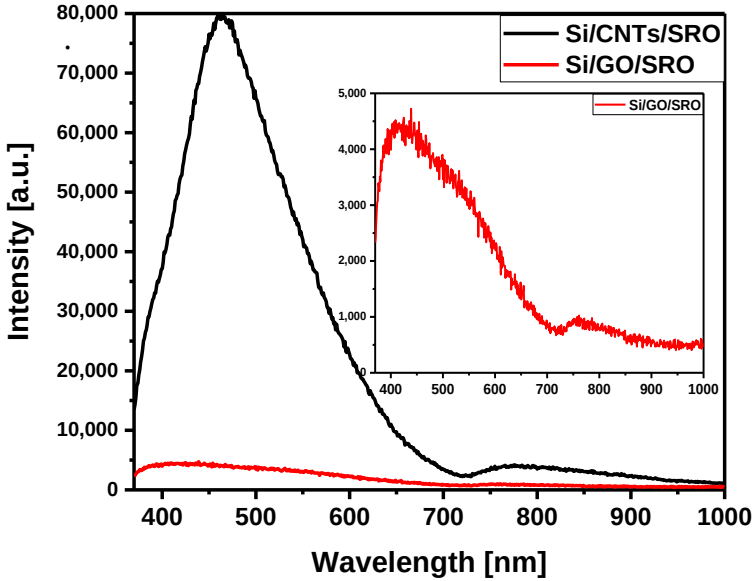

Graph 1. PL spectra of the Si/CNTs/SRO and Si/GO/SRO structures.

Graph 1 shows the photoluminescence spectrum of the Si/CNTs/SRO structure, and the inset shows the photoluminescence spectrum of the Si/GO/SRO structure. The PL intensity of the Si/CNTs/SRO structure shows a strong and well-defined peak in blue (450 nm), which is attributed to the CNTs, in addition, a lower intensity peak can be seen in the red band around 750 nm. For Si/GO/SRO structure two peaks appeared, a more defined peak around 420 nm was attributed to GO, just like in the structure with CNT, a smaller peak appeared around 750 nm, and this is a characteristic of SRO films.

Graph 2 shows the photoluminescence spectrum of the Si/GO-CNTs/SRO structure, and the inset shows the photoluminescence spectrum of the Si/CNTs-GO/SRO structure. The PL intensity of the Si/GO-CNTs/SRO structure shows a strong and clear green peak (519 nm), which is attributed to the existence of the GO-CNTs composite [11]. For the Si/CNTs-GO/SRO structure, two peaks are shown, a more defined peak around 400 nm is attributed to GO, and another weaker peak around 750 nm and as mentioned above, is characteristic of SRO films.

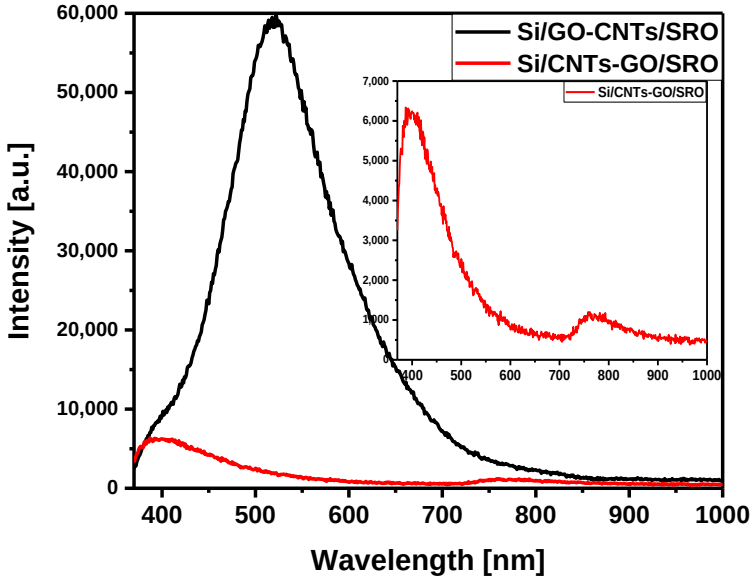

Graph 2. PL spectra of the Si/GO-CNTs/SRO and Si/CNTs-GO/SRO structures.

Results

As shown in Graphs 1 and 2, the photoluminescence spectrum is very broad, suggesting that multiple emission mechanisms may be involved. To find all possible contributions to the photoluminescence process in the structure, the deconvolution of each spectrum is shown in Graph 3.

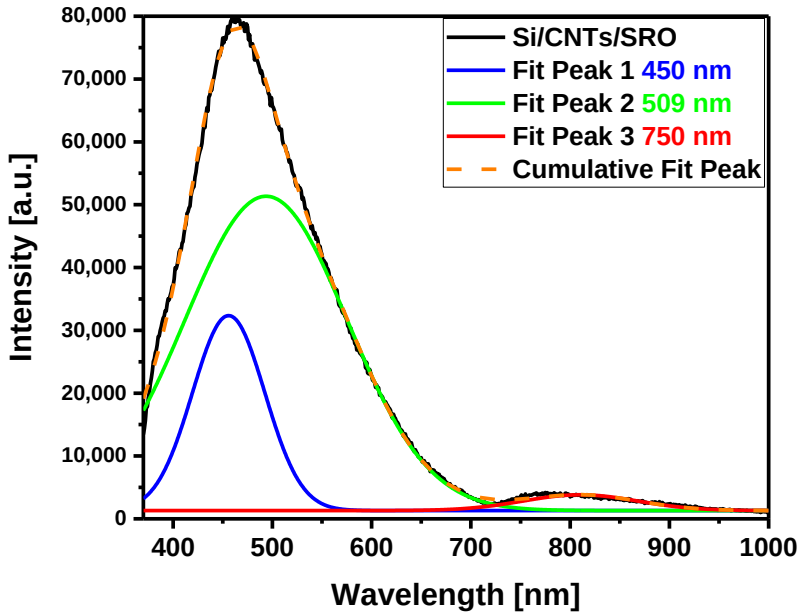

Graph 3. Deconvoluted spectra of the Si/CNTs/SRO structure.

The different peaks defined by the deconvolution are associated with different types of defects, as shown below, with their respective positions in energy, see Table 1.

CNTs/SRO photoluminescence emission mechanisms.	
Luminescent centers associated with diamond films	450 nm [11]
Defects due to Nitrogen	509 nm [12]
Nonbridging oxygen hole centers	750 nm [13]
GO/SRO photoluminescence emission mechanisms.	
It is attributed to the excimer present in the GO	405 nm [14]
Interactions between graphene planes and OD (Oxidative debris)	495 nm [14]
Nonbridging oxygen hole centers	750 nm [13]

Table 1. Types of defects linked to the position of the PL peaks of the structures.

Conclusions

The photoluminescence properties of CNTs, GO, and SRO thin film layers and heterostructures formed from these materials were investigated and compared. The photoluminescence spectra show the emission of CNTs in the blue-green region, which is thought to be caused by contamination caused by nitrogen binding to carbon in the blue region, and the characteristic green-emitting functional groups of CNTs due to C=O. GO emission was observed in two bands, 405 and 495 nm, caused by oxidative debris and excimers, respectively. Whereas for the SRO film, a contribution of 750 nm due to nonbridging oxygen hole centers is present. In the structure of mixed CNT and GO, the emission shift and its shielding are observed, which is due to the presence of nitrogen defects in the CNTs, whereas for the structure with GO on top, the emission is the same as that of GO without carbon nanotubes. Structures with CNTs have great potential in light-emitting device applications due to their good emission behavior.

References

[1] Martínez, H., Luna, J., Morales, R., Casco, J., Hernández, J., & Luna, A. et al. (2021). Blue Electroluminescence in SRO-HFCVD Films. *Nanomaterials*, *11*(4), 943. https://doi.org/10.3390/nano11040943

[2] Simón, Z., López, J., de la Luz, Á., Salgado, G., Leyva, K., & López, J. et al. (2021). SiOx films deposited by HFCVD: Their conduction response to light and intrinsic photovoltaic effect. *Surfaces And Interfaces*, *26*, 101411. https://doi.org/10.1016/j.surfin.2021.101411

[3] Hernández Simón, Z., Luna López, J., de la Luz, A., Pérez García, S., Benítez Lara, A., & García Salgado, G. et al. (2020). Spectroscopic Properties of Si-nc in SiOx Films Using HFCVD. *Nanomaterials*, *10*(7), 1415. https://doi.org/10.3390/nano10071415

[4] Martínez Hernández, H., Luna López, J., Hernández de la Luz, J., Luna Flores, A., Monfil Leyva, K., & García Salgado, G. et al. (2020). Spectroscopic and Microscopic Correlation of SRO-HFCVD Films on Quartz and Silicon. *Crystals*, *10*(2), 127. https://doi.org/10.3390/cryst10020127

[5] Avouris, P., Freitag, M., & Perebeinos, V. (2008). Carbon-nanotube photonics and optoelectronics. *Nature Photonics*, *2*(6), 341-350. https://doi.org/10.1038/nphoton.2008.94

[6] Cayuela, A., Soriano, M., & Valcárcel, M. (2015). Photoluminescent carbon dot sensor for carboxylated multiwalled carbon nanotube detection in river water. *Sensors And Actuators B: Chemical*, 207, 596-601. https://doi.org/10.1016/j.snb.2014.10.102.

[7] Lee, K., Wu, Z., Chen, Z., Ren, F., Pearton, S., & Rinzler, A. (2004). Single Wall Carbon Nanotubes for p-Type Ohmic Contacts to GaN Light-Emitting Diodes. *Nano Letters*, *4*(5), 911-914.https://doi.org/10.1021/nl0496522

[8] Montes-Navajas, P., Asenjo, N., Santamaría, R., Menéndez, R., Corma, A., & García, H. (2013). Surface Area Measurement of Graphene Oxide in Aqueous Solutions. *Langmuir*, *29*(44), 13443-13448. https://doi.org/10.1021/la4029904

[9] Han, J., Kim, J., Jo, S., Kim, S., Kim, J., & Kang, B. et al. (2012). Graphene oxide as a multi-functional p-dopant of transparent single-walled carbon nanotube films for optoelectronic devices. *Nanoscale*, *4*(24), 7735. https://doi.org/10.1039/c2nr31923c

[10] Jin, Y., Zheng, Y., Podkolzin, S., & Lee, W. (2020). Band gap of reduced graphene oxide tuned by controlling functional groups. *Journal Of Materials Chemistry C*, *8*(14), 4885-4894. https://doi.org/10.1039/c9tc07063j

[11] Fedoseeva, Y., Bulusheva, L., Okotrub, A., Kanygin, M., Gorodetskiy, D., & Asanov, I. et al. (2015). Field emission luminescence of nanodiamonds deposited on the aligned carbon nanotube array. *Scientific Reports, 5*(1). https://doi.org/10.1038/srep09379

[12] Zhou, J., Zhou, X., Li, R., Sun, X., Ding, Z., Cutler, J., & Sham, T. (2009). Electronic structure and luminescence center of blue luminescent carbon nanocrystals. *Chemical Physics Letters, 474*(4-6), 320-324. https://doi.org/10.1016/j.cplett.2009.04.075

[13] Vaccaro, L., Cannas, M., & Radzig, V. (2009). Luminescence properties of nonbridging oxygen hole centers at the silica surface. *Journal Of Non-Crystalline Solids*, *355*(18-21), 1020-1023. https://doi.org/10.1016/j.jnoncrysol.2008.11.028

[14] Du, D., Song, H., Nie, Y., Sun, X., Chen, L., & Ouyang, J. (2015). Photoluminescence of Graphene Oxide in Visible Range Arising from Excimer Formation. *The Journal Of Physical Chemistry C, 119*(34), 20085-20090. https://doi.org/10.1021/acs.jpcc.5b04529

ECORFAN®